Journal of ELECTRONIC MATERIALS, Vol. 46, No. 10, 2017
DOI: 10.1007/s11664-017-5630-6

Functionalized Multiwalled Carbon Nanotube Electrochemical Sensor for Determination of Anticancer Drug Flutamide

JULIANNA SANTOS FARIAS,[1] HUDSON ZANIN,[2] ADRIANA SILVA CALDAS,[1] CLENILTON COSTA DOS SANTOS,[3] FLAVIO SANTOS DAMOS,[1] and RITA DE CÁSSIA SILVA LUZ [1,4]

1.—Laboratory of Sensors, Devices and Analytical Methods, Department of Chemistry, Federal University of Maranhão, Av. dos Portugueses 1966, São Luís, MA CEP: 65080-805, Brazil. 2.—Carbon Sci-Tech Labs, School of Electrical and Computer Engineering, University of Campinas, Av Albert Einstein 400, Campinas, SP 13083-852, Brazil. 3.—Department of Physics, Federal University of Maranhão, Av. dos Portugueses 1966, São Luís, MA CEP: 65080-805, Brazil. 4.—e-mail: rita.luz@ufma.br

An electrochemical sensor based on functionalized multiwalled carbon nanotubes ($MWCNT_f$) has been developed and applied for determination of anticancer drug flutamide in pharmaceutical and artificial urine samples. The electrode was prepared by modifying a glassy carbon electrode with $MWCNT_f$, denoted herein as $MWCNT_f$/GCE. The $MWCNT_f$/GCE electrode exhibited high catalytic activity, high sensitivity, and high stability and was applicable over a wide concentration range for flutamide. The effects of the scan rate, pH, and nature of the electrolyte on the electrochemical behavior of flutamide on the $MWCNT_f$/GCE were investigated. The results showed that this electrode presented the best square-wave voltammetric response to flutamide in Britton–Robinson buffer solution at pH 5.0 at frequency of 50 Hz and amplitude of 0.06 V. The proposed sensor presents a wide linear response range from concentration of 0.1 μmol L^{-1} up to 1000 μmol L^{-1} (or 27.6 μg L^{-1} up to 0.27 g L^{-1}), with limit of detection, limit of quantification, and sensitivity of 0.03 μmol L^{-1}, 0.1 μmol L^{-1}, and 0.30 μA μmol^{-1} L, respectively. The $MWCNT_f$/GCE electrode was successfully applied for determination of flutamide in pharmaceutical formulations and artificial urine samples, giving results in agreement with those obtained by a comparative method described in literature. A paired Student's *t*-test revealed no statistical difference between the reference and proposed method at 95% confidence level. The average recovery for fortified samples was 101 ± 1%.

Key words: Flutamide, functionalized multiwalled carbon nanotubes, electrochemical sensor, pharmaceutical samples, urine samples

INTRODUCTION

Nowadays, development of methods for determination of drugs is a challenging topic in scientific research since drug monitoring in biological, pharmaceutical, environmental, and food samples is of great importance for monitoring of diseases and quality control of pharmaceutical dosages and foods. In this context, biological fluids such as urine are promising samples for drug monitoring, due to their ready availability and noninvasive collection in comparison with blood, serum, amniotic fluid, gastric contents, or specific tissues, among others.[1] On the other hand, monitoring of drugs in pharmaceutical formulations is of great importance in the pharmaceutical industry as well as to ensure the safety of patients treated with them.

Flutamide, i.e., 2-methyl-*N*-[4-nitro-3-(trifluoromethyl)phenyl]propanamide (Fig. 1), is a nonsteroidal antiandrogen drug used to treat advanced

(Received December 6, 2016; accepted May 31, 2017; published online June 15, 2017)

prostate cancer. In addition, flutamide may also be used to treat excess androgen levels in women with polycystic ovarian syndrome.[2,3] In prostate cancer, tumor cells need testosterone to proliferate; flutamide and its active metabolite, 2-hydroxyflutamide, compete with testosterone to bind to androgen receptors, leading to impairment of testosterone signaling.[4]

However, the efficacy of flutamide is somewhat overshadowed by the occurrence of hepatitis in some patients,[5] which increases the importance of flutamide monitoring in urine samples as well as drug formulations used in patients with prostate cancer. Therefore, development of a simple, sensitive, and selective method for determination of flutamide in routine analysis is of great importance.

There are several methods for determination of flutamide, including spectrophotometric approaches,[6] chemiluminescence-based methods,[7] and high-performance liquid chromatography (HPLC).[8] Although these methods show good sensitivity and accuracy, they suffer from high operational cost and require specific sample preparation as well as highly trained technicians.

On the other hand, electrochemical methods have received great attention due to their various advantages, including low operational cost, high sensitivity, high frequency of analysis, and easy handling. Conventional applications involving electroanalytical methods are based on electrodes whose usefulness may be limited due to gradual passivation of the surface,[9] slow electron transfer kinetics, high potential for oxidation/reduction of the analyte, and difficulty in discriminating between target compounds with similar redox characteristics.[10]

Chemical modification of electrodes can help to address these problems, giving rise to electrodes with interesting physicochemical characteristics such as reactivity, selectivity, sensitivity, etc. Such chemically modified electrodes enable development of devices with responses appropriate for different purposes and applications.[11] In this sense, electrochemical sensors based on modified electrodes have opened new avenues in several areas of research, enabling detection and quantification of substances using different materials.[12,13] Among the various materials used nowadays in development of chemical sensors, carbon nanotubes (CNTs) stand out due to their chemical and mechanical properties, chemical stability, and robustness.[14]

There is therefore growing interest in use of carbon nanotubes as a platform for development of sensors for determination of drugs in pharmaceutical formulations or biological samples, based on two main aspects: Firstly, CNTs show excellent electrochemical activity,[15] motivating their use for determination of drugs with high sensitivity and allowing low limits of detection for many drugs in pharmaceutical samples; Secondly, the high number of groups on the surface of carbon nanotubes enables higher selectivity. Based on these aspects, carbon

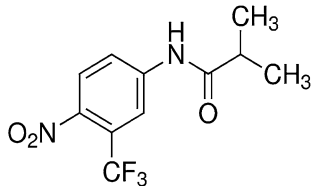

Fig. 1. Chemical structure of flutamide.

nanotubes have been employed for determination of drugs such as dopamine,[16] quercetin,[17] methamphetamine,[18] ascorbic acid,[19] nimesulide,[20] paracetamol,[21] norfloxacin,[22] bisoprolol fumarate,[23] oxymetholone,[24] valganciclovir,[25] warfarin,[26] captopril,[27] methadone,[28] isoprenaline,[29] morphine,[30] noscapine,[31] ceftazidime,[32] L-tryptophan,[33] cefpirome,[34] and gentamicin sulfate,[35] among others.

To improve the properties of CNTs, they can be functionalized by attaching carboxylic and other oxygen-containing polar groups using oxygen plasma treatment, which has been crucial for adsorption processes to transform the surface of CNTs from superhydrophobic to superhydrophilic.[36] In this work, we developed, applied, and validated a functionalized-CNT-modified electrode for determination of flutamide in pharmaceutical samples and artificial urine samples. To the best of the authors' knowledge, this is the first description of such a high-performance nanomaterial based on functionalized multiwalled carbon nanotubes for determination of flutamide.

EXPERIMENTAL PROCEDURES

Chemicals, Solutions, and Instrumentation

All chemicals were of analytical grade and used as received without further purification steps. Flutamide and dimethylformamide (DMF) were acquired from Sigma, St. Louis, USA. Boric acid, citric acid, and disodium and monosodium phosphate (Na_2HPO_4 and NaH_2PO_4) were acquired from Synth, São Paulo, Brazil. Urea, sodium chloride, creatinine, and calcium chloride dihydrate were purchased from Isofar, Rio de Janeiro, Brazil.

Working standard solutions were prepared daily by appropriate dilution of stock solutions. All solutions were prepared using water purified in a Milli-Q Millipore system, and the actual pH of the buffer solutions was determined using a Quimis pH/ion analyzer Q400AS model. Britton–Robinson (B–R) buffer solution (0.1 mol L^{-1}) was prepared by mixing acetic acid, boric acid, and orthophosphoric acid solutions with an appropriate amount of sodium hydroxide solution to adjust the pH. McIlvein buffer solution (0.1 mol L^{-1}) was prepared from 0.1 mol L^{-1} Na_2HPO_4, and the pH was adjusted using 1 mol L^{-1} citric acid.

A PGSTAT 128 N potentiostat/galvanostat from Autolab (Eco Chemie) was coupled to a microcomputer and controlled using GPES software. The

electrochemical cell was a conventional three-electrode cell with Ag/AgCl(sat.) reference electrode, gold auxiliary electrode, and (bare or modified) glassy carbon (GC) working electrode.

Synthesis and Functionalization of Multiwalled Carbon Nanotubes (MWCNT)

MWCNT were prepared using a mixture of camphor (85 wt.%) and ferrocene in a modified thermal chemical vapor deposition (CVD) furnace. The mixture was vaporized at 220°C in an antechamber, then the vapor was carried by nitrogen gas flow to the chamber of the CVD furnace set at 850°C and atmospheric pressure. The vapors flowing into the chamber were converted into MWCNT powder.[37] The time elapsed during this process was only a few minutes. After preparation, the samples were subjected to sonication for 5 h in 10 mol L^{-1} HCl at 150°C, then washed extensively in water and left to dry. Acid etching was performed to remove iron-based (from ferrocene) catalytic particles from the MWCNT powder.[38] We reported previously that, based upon x-ray photoelectron spectroscopy (XPS) analysis, this process succeeded in almost complete removal of external iron content.[38,39]

Finally, exfoliation of the carbon nanotubes and incorporation of oxygen-containing groups (−OH, −COOH, =O) were performed in a pulsed direct-current (DC) plasma reactor at oxygen flow rate of 1 sccm, pressure of 150 mTorr, −700 V, and frequency of 20 kHz. After this functionalization of the MWCNT, we denote them by $MWCNT_f$.

Sensor Preparation

First, the surface of the glassy carbon electrode was polished to remove any adsorbed species. Then, the glassy carbon electrode was modified with 10 μL of a suspension prepared by mixing 1.0 mg $MWCNT_f$ and 500 μL DMF. This suspension was placed directly onto the glassy carbon electrode surface and allowed to dry at 50°C for 20 min. The modified electrode is denoted as $MWCNT_f$/GCE. Finally, the modified electrode was thoroughly rinsed with distilled water and transferred to the electrochemical cell.

Preparation of Pharmaceutical and Synthetic Urine Samples

Six tablets containing 250 mg flutamide were accurately weighed and ground to fine powder. Tablet powder equivalent to 250 mg flutamide was weighed accurately and dissolved in ethyl acetate. The solution was filtered and transferred quantitatively to a 100-mL volumetric flask, and the volume was completed with the same solvent. An aliquot of 10 μL of each sample was added to the electrochemical cell containing 5 mL 0.1 mol L^{-1} B–R buffer (pH 5.0) for analysis. The same procedure was also carried out in triplicate, with the sample diluted 500 times (10 μL sample/5 mL electrolyte). This method was also applied for direct analysis of flutamide in two different artificial urine samples, prepared as follows:

Procedure for sample A: Artificial urine was prepared in water with the following constituents and final concentrations: 0.33 mol L^{-1} urea, 0.12 mol L^{-1} sodium chloride, 0.016 mol L^{-1} potassium diphosphate, 0.007 mol L^{-1} creatinine, and 0.004 mol L^{-1} sodium monophosphate.[40]

Procedure for sample B: Artificial urine was prepared according to Laube et al.[41] as a solution containing the following constituents and final concentrations: 0.411 mol L^{-1} urea, 0.0268 mol L^{-1}, potassium chloride, 3 g L^{-1} sodium chloride, 0.0513 mol L^{-1} sulfate disodium, 0.014 mol L^{-1} potassium phosphate, 0.0186 mol L^{-1} ammonium chloride, and 0.0068 mol L^{-1} calcium chloride dihydrate. In both procedures, the pH of the sample solution was 6.6 (±0.1).

RESULTS AND DISCUSSION

$MWCNT_f$ Characterization

The details of the $MWCNT_f$ characterization were reported elsewhere.[38,39] Briefly here, Fig. 2a shows the morphological characterization of $MWCNT_f$ performed by scanning electron microscopy (SEM), and Fig. 2b shows the first- and second-order Raman spectrum of the $MWCNT_f$ sample. Curve fitting was performed using Lorentzian functions for the D (1350 cm^{-1}) and G bands (1580 cm^{-1}) and D′ shoulder (1618 cm^{-1}), and Gaussian functions for the broad band around 1474 cm^{-1}, which is assigned to polar groups attached to the CNT walls. The D band stems from a double resonance process involving a phonon and a defect. The G band stems from in-plane vibrations and has E_{2g} symmetry corresponding to stretching vibrations in the basal plane (sp^2 domains) of single-crystal graphene or nanocrystalline graphite. The G′ band (2700 cm^{-1}) is derived from their (2D) second-order harmonic. The higher the intensity of the G′ band, the higher the crystallinity of the sp^2 carbon.[38,39] The C 1*s* curves were deconvoluted into six peaks, at around 284.1 eV, 285.4 eV, 287.1 eV, 288.7 eV, 290.1 eV, and 291.6 eV, corresponding to aliphatic carbons (sp^2 hybridization), defects, carbon atoms with C–O, –C=O, carbonates, and shake-up peak (π–π^* transitions), respectively.

From the C 1*s* curves, we observed an increase of both oxygen-group content and defects, in agreement with the Raman spectra. This implies formation of strong C–O bonds from the oxygen-containing groups situated along the carbon nanotubes. The O 1*s* curves were deconvoluted into three peaks at around 535 eV, 534 eV, and 531 eV, corresponding to C–O, –COOH, and C–OH.

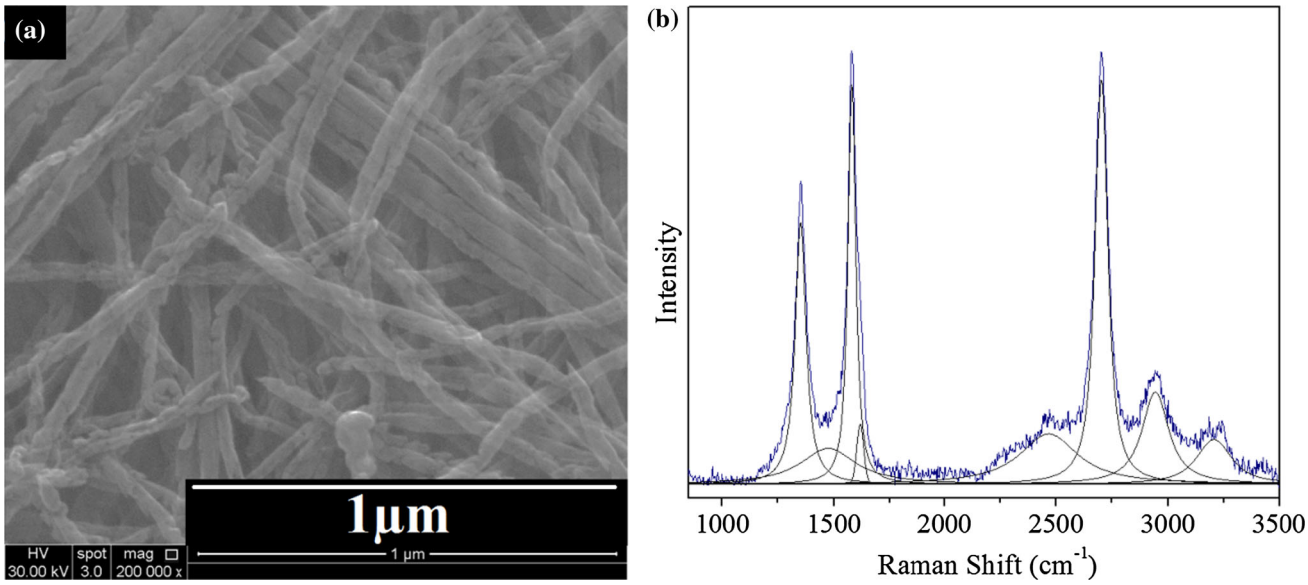

Fig. 2. (a) SEM and (b) Raman spectrum of $MWCNT_f$.

Electrochemical Studies of Flutamide on $MWCNT_f$/GCE

The electrochemical behavior of flutamide on the bare GCE (Fig. 3a) and $MWCNT_f$/GCE (Fig. 3b) was studied in phosphate buffer solution (PBS, pH 7). Curves 1 (first cycle) and 2 (second cycle) in Fig. 3a show results of cyclic voltammetry (CV) performed in the anodic scan, while curves 3 (first cycle) and 4 (second cycle) in Fig. 3a show the results of CV carried out in the cathodic scan. In both cases, CV shows one oxidation peak (OI) at +120 mV and two cathodic peaks (RI and RII) at −660 mV and −140 mV, respectively. The RI peak is due to four-electron reduction of the nitro group of flutamide on the electrode surface.[42] On the other hand, the redox couple OI/RII can be attributed to reversible two-electron oxidation/reduction of the hydroxylamine group [(–NHOH)/nitroso group (–NO)].[42,43] It is noteworthy that the RII peak appears only after the first cycle is performed (Fig. 3a, curve 4).

On the other hand, the CV results for flutamide oxidation/reduction on $MWCNT_f$ (Fig. 3b, curves 1 to 4) show the OI peak at −34 mV and the RII peak at −89 mV, while the RI peak appears at −600 mV. The difference between the potential of peaks OI and RII ($E_{OI} - E_{RII}$) was +55 mV. In addition, in the cathodic scan, the OI/RII redox couple disappeared when the potential was reversed before the RI peak was reached (data not shown), consistent with the nitroso/hydroxylamine redox couple of flutamide being generated by reduction of nitro group of flutamide.

Figure 3c presents CV results for flutamide oxidation/reduction on bare GCE (curve 1) and $MWCNT_f$/GCE (curve 2) at the same experimental conditions. These results show that the flutamide redox processes were more efficient on the $MWCNT_f$-modified electrode. The peak currents observed for the OI/RII redox couple in Fig. 3c (curve 2) are about 3-fold higher than that on bare GCE (Fig. 3c, curve 1).

These results suggest low charge-transfer resistance of the $MWCNT_f$ electrode to flutamide due to the greater amount of surface groups resulting from its oxidized structure, which increased the sensitivity of the system and improved the electron transfer rate between the analyte in solution and the electrode surface. The peak currents of flutamide oxidation/reduction on $MWCNT_f$/GCE were markedly higher than those on bare GCE, suggesting that $MWCNT_f$ is an effective mediator in electroanalysis of flutamide. In addition, the peak potentials for flutamide oxidation and reduction on $MWCNT_f$/GCE were lower than those observed on bare glassy carbon electrode. The enhancement of the peak current of the redox couple and the shift toward lower values indicate that $MWCNT_f$ exhibits effective catalytic ability to oxidize or reduce flutamide.

Figure 4 shows cyclic voltammograms for $MWCNT_f$-modified glassy carbon electrode at several flutamide concentrations (0.1 mmol L^{-1}, 0.2 mmol L^{-1}, 0.3 mmol L^{-1}, and 0.4 mmol L^{-1}) in two potential ranges (Fig. 4a and b). The peak currents observed for flutamide oxidation and reduction on the $MWCNT_f$-modified glassy carbon electrode were proportional to the concentration of the electroactive species in the buffer solution, which occurs due to the arrival of a greater amount of molecules at the electrode–solution interface.

According to these results, in both ranges, the peak currents increased with the flutamide concentration and the plots of peak (anodic and cathodic) currents as functions of the flutamide concentration

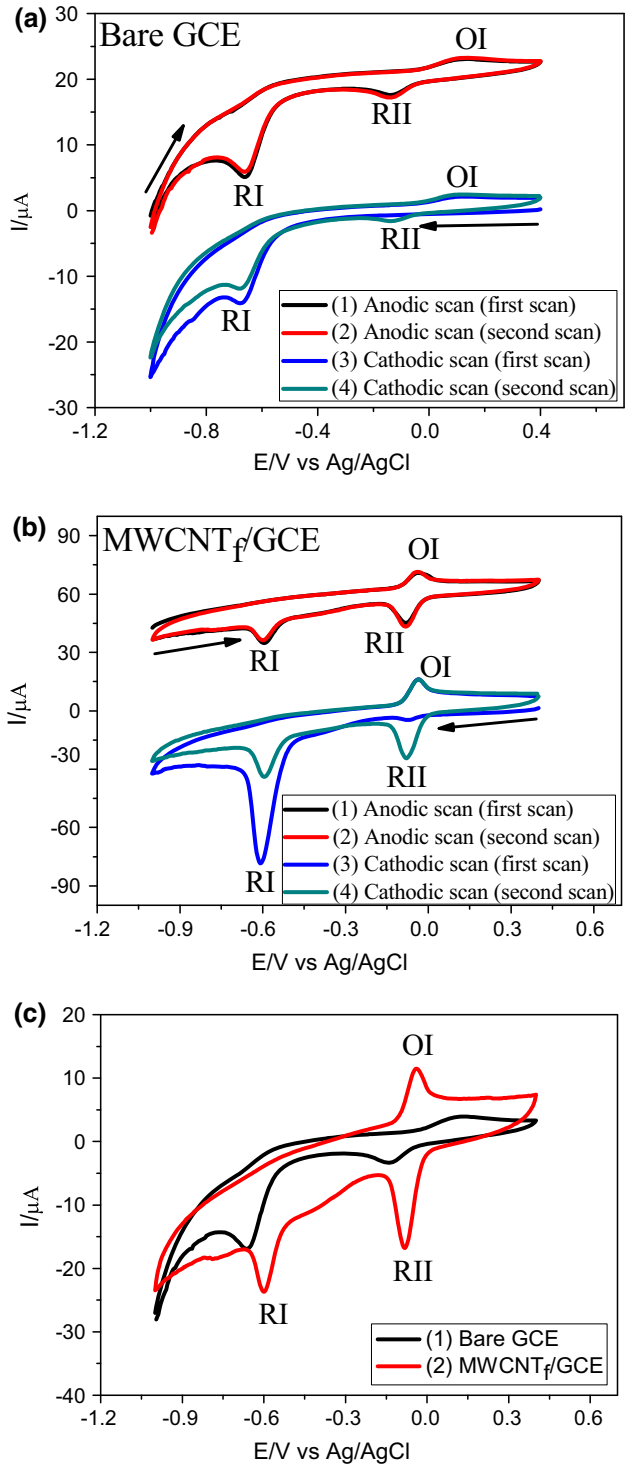

Fig. 3. CV results for flutamide on: (a) bare GCE and (b) $MWCNT_f$/GCE. The two figures show anodic (red and black) and cathodic (blue and green) scans of the first and second cycle, respectively. (c) CV results for oxidation of flutamide on bare GCE (black curve) and $MWCNT_f$/GCE (red curve). Experiments were carried out in 0.1 mol L^{-1} PBS at pH 7.0 (Color figure online).

were linear, suggesting the applicability of the modified sensor for detection of flutamide. However, the cathodic peak near to 0 V (peak RII) was chosen for flutamide determination in further experiments,

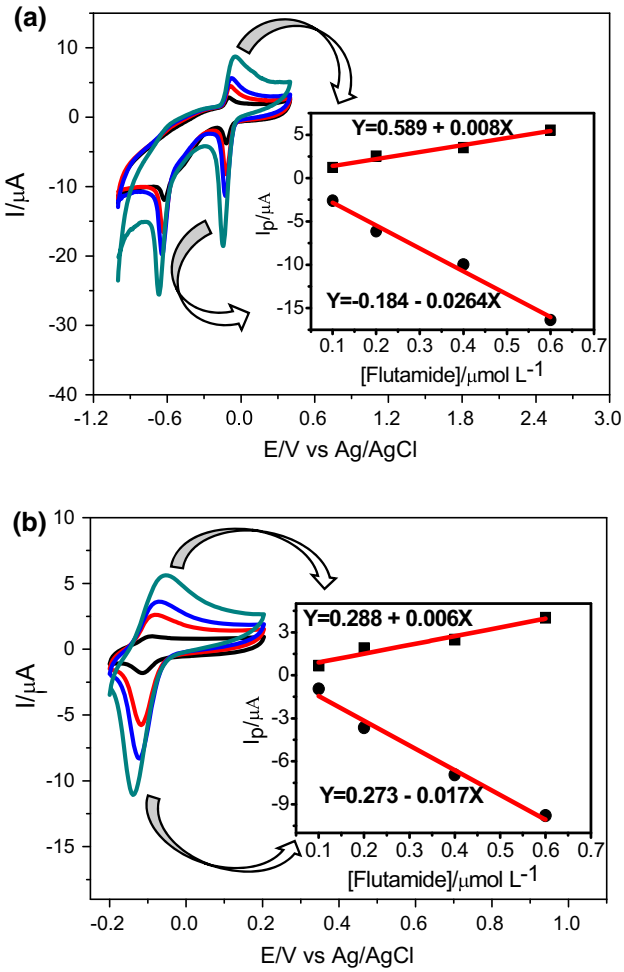

Fig. 4. CV results for $MWCNT_f$/GCE in presence of different concentrations of flutamide: (a) potential scan between −1.0 V and 0.4 V with inset showing plot of I_p versus [flutamide]; (b) potential scan between −0.2 V and 0.2 V with inset showing plot of I_p versus [flutamide].

since it provided high sensitivity at low applied potential.

Optimization of Experimental and Operational Parameters for Determination of Flutamide

Experimental Parameters

To optimize the sensor response for flutamide determination, the influence of experimental parameters was investigated by cyclic voltammetry (Fig. 5). Firstly, the effects of solution pH on the sensor response to flutamide was studied in 0.1 mol L^{-1} phosphate buffer at pH values of 4.0, 5.0, 6.0, and 7.0 (Fig. 5a). The inset of Fig. 5a shows a plot of E_p (peak potential) versus pH, obtained to verify the chemical order of protons to electrons for oxidation and reduction of flutamide. The peak potential for flutamide was affected by the solution pH in the investigated range. A linear relationship between the peak potential and pH in the range of

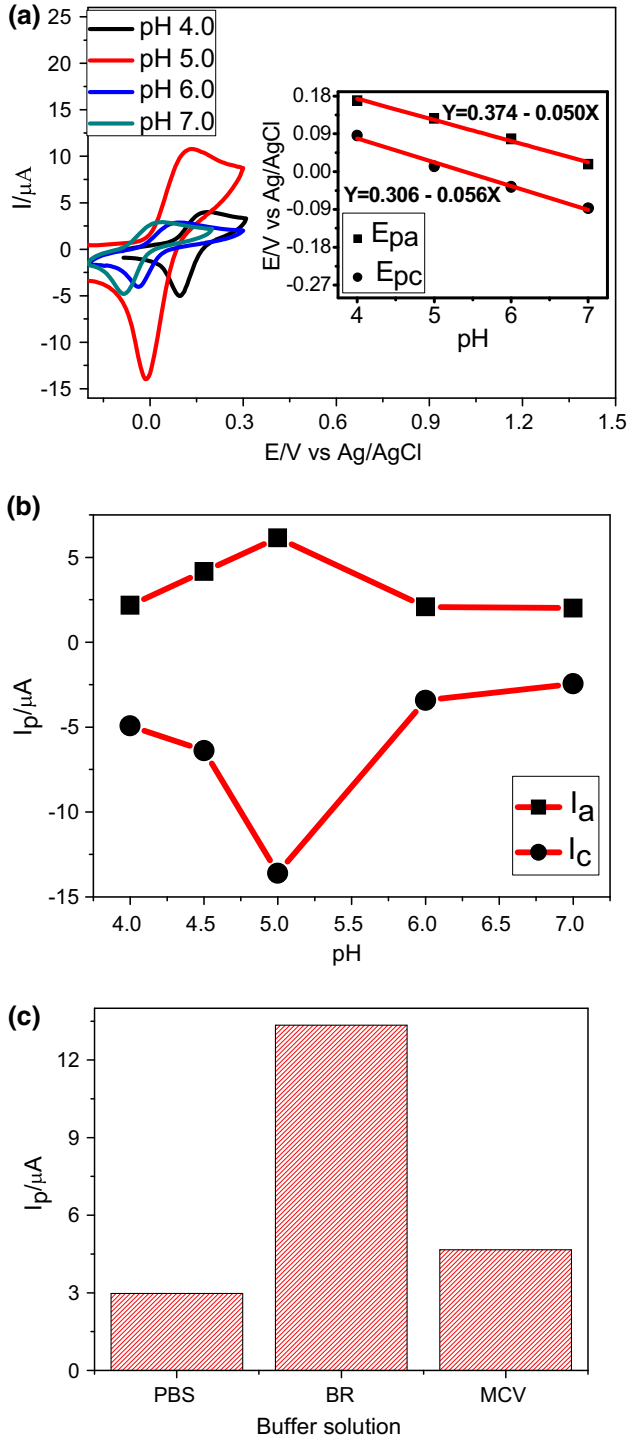

Fig. 5. (a) CV results for flutamide on MWCNT$_f$/GCE at different solution pH values of 4.0, 5.0, 6.0, and 7.0, measured in 0.1 mol L^{-1} PBS buffer (pH 5.0); inset shows plot of E_p versus pH. (b) Influence of pH on peak current of flutamide, obtained from (a), and (c) influence of type of buffer solution on the peak current of flutamide, measured in 0.1 mol L^{-1} buffer (pH 5.0) using CV technique. [Flutamide] = 0.4 mmol L^{-1}; scan rate: 0.05 V s^{-1}.

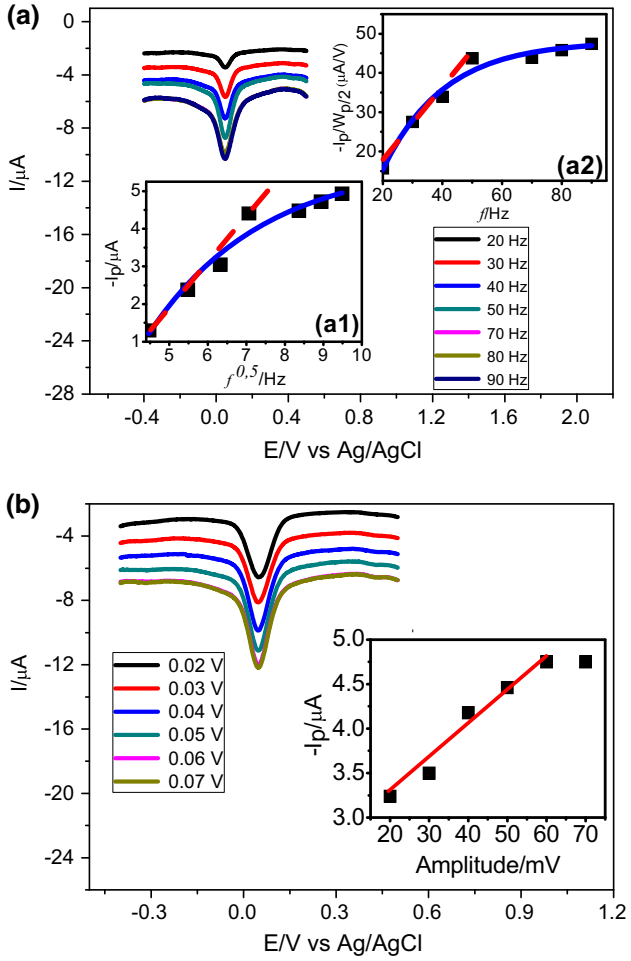

Fig. 6. Dependence of peak current on (a) square-wave voltage (SWV) frequency (with A_p = 0.05 V) and (b) pulse amplitude. Inset a1 shows a plot of peak current versus square root of frequency. Inset a2 shows a plot of peak current normalized to half-peak width. The inset in (b) shows a plot of peak current versus amplitude. Experiments were carried out under the following conditions: [flutamide] = 10 μmol L^{-1} in B–R buffer (pH 5.0).

pH 4.0–7.0 was observed for the flutamide oxidation/reduction process, with slope of 0.053 V/pH, close to that expected for an electrode reaction in which the number of protons is equal to the number of electrons (0.059 V/pH at 25°C).[44] We then verified that the peak current also depended on the solution pH. The results showed that the peak current for flutamide increased from pH 4.0 up to pH 5.0, decreased from pH 5.0 up to pH 6.0, then remained constant up to pH 7.0 (Fig. 5b). The highest peak current was achieved at pH 5.0, which was therefore chosen for further studies.

The effect of the buffer solution on the peak current obtained with the sensor for flutamide was also investigated (Fig. 5c). Thus, the sensor response was verified in three different buffer solutions [phosphate (PBS), Britton–Robinson (B–R), and McIlvaine (MCV)] at 0.1 mol L^{-1} and pH 5.0. The best response to flutamide was found in B–R buffer, which may be associated with the high ionic mobility of the acetate, phosphoric, and boric ions, enabling better electron transfer between the

electrode and flutamide in solution. B–R buffer was therefore chosen for further experiments.

Operational Parameters

The effect of the frequency (f) and potential pulse amplitude (A_p) on the square wave voltammetric response of flutamide on $MWCNT_f$/GCE in B–R solution is shown in Fig. 6a and b. The peak current values increased linearly with the square root of frequency from 20 Hz up to 50 Hz (Fig. 6a, inset a1). On the other hand, the deviation of the peak current values from linearity increased when the frequency was increased, being higher at frequency values above 50 Hz (Fig. 6a, inset a1). Inset a2 of Fig. 6a shows a plot of peak current normalized to the half-peak width ($I_p/W_{p/2}$) versus frequency, also revealing linear behavior up to frequency of 50 Hz, which suggests that the increase of the peak current was accompanied by an increase of the half-peak width. According to literature,[45] increasing the frequency can induce an increase of the half-peak width due to (i) effects on the uncompensated resistance or (ii) limited diffusion of flutamide to the $MWCNT_f$/GCE surface. Taking into account that the resolution is a reasonable criterion for the quality of a square-wave peak as an analytical signal, a frequency of 50 Hz was used for further experiments as a trade-off between the advantage of an increase in the peak current versus the accompanying peak broadening.

The values of the peak current were also found to vary with the pulse amplitude (0.02 V to 0.07 V) applied in the SWV while maintaining a frequency of 50 Hz (Fig. 6b). The results showed that there was no change in the peak current for amplitude values above 0.06 V. In this sense, better voltammetric response was obtained for pulse amplitude of 0.06 V, which was therefore chosen for further studies.

Analytical Characterization

To obtain an analytical curve for the proposed sensor, we measured SW voltammograms for reduction of flutamide at different concentrations in 0.1 mol L^{-1} B–R buffer at pH 5.0 under the optimized experimental conditions (Fig. 7). Under the optimized conditions, the proposed sensor showed a typical linear response range from 0.1 μmol L^{-1} up to 1000 μmol L^{-1}, which can be expressed according to the following equation: $Y = (1.026 \pm 0.650) + (0.30 \pm 0.002)X$, with $r^2 = 0.999$ (n = 15), with better sensitivity than reported by other researchers (Table I). This good sensitivity can be attributed to the efficiency of the electron transfer between the $MWCNT_f$ and the flutamide.

A limit of detection of 0.03 μmol L^{-1} was determined using a 3σ/slope ratio, while the limit of quantification was 0.10 μmol L^{-1}, where σ is the standard deviation of the mean value for ten voltammograms of blank, calculated according to

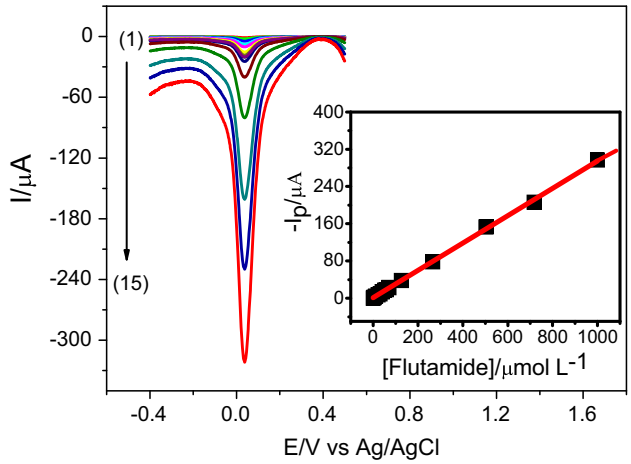

Fig. 7. SWV flutamide reduction obtained in B–R buffer (pH 5.0). The concentrations in the electrochemical cell were: (1) 0.1 μmol L^{-1}, (2) 2.4 μmol L^{-1}, (3) 4.8 μmol L^{-1}, (4) 10.2 μmol L^{-1}, (5) 22.0 μmol L^{-1}, (6) 31.0 μmol L^{-1}, (7) 40.9 μmol L^{-1}, (8) 51.0 μmol L^{-1}, (9) 58.0 μmol L^{-1}, (10) 70.0 μmol L^{-1}, (11) 126.0 μmol L^{-1}, (12) 265.0 μmol L^{-1}, (13) 503.0 μmol L^{-1}, (14) 718.0 μmol L^{-1}, and (15) 1000 μmol L^{-1}. Inset shows analytical curve. f = 50 Hz, pulse amplitude = 0.06 V.

literature recommendations.[46] The response range and limit of detection presented by this sensor for flutamide determination are better than those reported in literature (Table I).

The repeatability of the sensor construction was evaluated by constructing five sensors and determining the peak current obtained for each. The repeatability, expressed as the relative standard deviation (RSD), was 0.06% for n = 10. This result indicates good repeatability of sensor construction, possibly due to strong adsorption of the $MWCNT_f$ on the electrode surface.

The stability of the $MWCNT_f$/GCE electrode was also checked in the presence of 10 μmol L^{-1} flutamide by performing successive voltammetric amperometric measurements in 0.1 mol L^{-1} B–R buffer at pH 5.0. After 100 voltammetric measurements, no change was observed in the response of the modified electrode. When the modified electrode was stored at room temperature, no significant change in the response was observed over a period of 1 month.

Application to Samples

The proposed sensor was also applied for flutamide determination in two drug samples and two artificial urine samples. Determination of flutamide in the samples was carried out in 5.0 mL 0.1 mol L^{-1} B–R buffer (pH 5) containing 10 μL sample. Successive injections of standard flutamide solution into B–R buffer were performed for determination of the analyte in the samples. The concentration of flutamide in the drug and artificial urine samples is presented in Table II, which also shows a comparison between the proposed and a comparative method.

Table I. Comparison of some characteristics of various modified electrodes for detection of flutamide

Electrode	E_{red} (V)	Linear range (μmol L^{-1})	Sensitivity (μA μmol^{-1} L)	LOD (μmol L^{-1})	Ref.
Nano-Ag/MGCEs	−0.30 (versus SCE)	10–100 100–1000	4.5×10^{-6} 1.0×10^{-6}	9.33	47
dsDNA/CPE	−0.75 (versus SCE)	72.4–579	0.011	3.62	48
CTAB/CPE	−0.75 (versus Ag/AgCl)	72.4–579	9.08×10^{-3}	0.181	49
Modified PGE	−0.25 (versus Ag/AgCl)	0.0001–0.1 0.1–100	1.24×10^{-5} 0.0043	34.4×10^{-6}	50
Dropping mercury electrode	0.55 (versus Ag/AgCl)	0.1–1.3	–	0.18	51
$MWCNT_f$	0.05 (versus Ag/AgCl)	0.1–1000	0.30	0.03	This work

LOD, limit of detection; MGCEs, modified glassy carbon electrodes; SCE, saturated calomel electrode; dsDNA, double-stranded deoxyribonucleic acid; CPE, carbon paste electrode; CTAB, cetyltrimethylammonium bromide; PGE, pencil graphite electrode.

Table II. Flutamide recovery values obtained for four samples (n = 6)

			Electrochemical method		Spectrophotometric method[52]	
Sample	Flutamide added (mg)	Flutamide expected (mg)	Flutamide found (mg)	Recovery (%)	Flutamide found (mg)	Recovery (%)
Tablets A	0.00	250.00	249.90 (±1.00)	99.9	251.50 (±1.20)	100.6
	10.00	260.00	253.54 (±0.50)	97.5	252.27 (±0.70)	99.4
Tablets B	0.00	250.00	249.7 (±0.30)	99.8	248.48 (±0.50)	99.5
	20.00	270.00	285.26 (±0.20)	105.6	284.93 (±0.40)	99.9
Artificial urine A	0.00	–	–	–	–	
	10.00	10.00	9.99 (±0.02)	99.00	9.75 (±0.02)	97.5
	20.00	20.00	19.87 (±0.10)	98.70	19.98 (±0.10)	100.6
Artificial urine B	0.00	–	–	–	–	–
	10.00	10.00	9.97 (±0.05)	97.00	9.99 (±0.12)	100.2
	20.00	20.00	19.95 (±0.03)	99.50	19.86 (±0.30)	99.5

Table III. Determination of flutamide in presence of excipients and other substances

Species	Amount (mmol L^{-1})	Recovery of Flutamide (% ± RSD[a])
Lactose monohydrate	10	98.8% (±0.5)
Magnesium stearate	10	99.1% (±0.3)
Sodium laureate	10	98.3% (±0.4)
Cellulose	10	97.7% (±0.8)
Amide	10	98.5% (±0.5)
Glucose	10	98.9% (±0.1)
Ascorbic acid	10	99.6% (±0.3)
Dextrose	10	100.5% (±0.5)
Talc	10	99.1% (±0.2)
Uric acid	10	99.7% (±0.1)
Vitamin B6	10	98.6% (±0.5)

[Flutamide] = 10 μmol L^{-1}.[a]Average of three determinations.

As an additional check on the accuracy of the developed method and interference by matrices, analytical recovery experiments were performed by adding known amounts of flutamide to three water samples in triplicate. Percentage recovery values were calculated by comparing the concentration obtained from the samples with the actual and added concentrations. The recoveries for the water samples are presented in Table II, clearly showing that the matrix had no influence on the developed sensor. A paired Student's *t*-test comparing the reference method and the results obtained using the proposed sensor revealed no statistical difference at 95% confidence level.

The selectivity of the modified electrode was evaluated by examining the influence of several possible interfering substances on the detection of 10 μmol L^{-1} flutamide in drug and urine samples. Solutions of these compounds were freshly prepared in the same conditions as flutamide, i.e., 0.1 mol L^{-1} B–R buffer (pH 5.0). The electrochemical results (Table III) indicated that 1000-fold higher concentrations of different species (lactose monohydrate, magnesium stearate, sodium laureate, cellulose, amide, glucose, ascorbic acid, dextrose, talc, uric acid, and vitamin B6) did not interfere with the flutamide determination. It is therefore apparent that, by exploiting the reduction of these species, the $MWCNT_f$-modified electrode can provide good selectivity for detection of flutamide, without interference from commonly coexisting substances. Therefore, the proposed sensor was highly selective for flutamide determination in the presence of excipients commonly present in tablets or electroactive compounds commonly found in urine samples.

CONCLUSIONS

This work shows that a glassy carbon electrode modified with $MWCNT_f$ is a simple, easily prepared, and practicable alternative for analytical determination of flutamide. Due to the chemical stability, electrochemical reversibility, and high electron transfer rate constant of the electrode, it can be used in electrocatalysis as an electron transfer mediator to shuttle electrons between flutamide and the electrode. This system has been shown to be promising for flutamide detection at extreme low overpotential, offering many desirable properties including low detection limit, satisfactory linear concentration range, and excellent stability. The sensor was successfully applied for drug and artificial urine samples.

ACKNOWLEDGEMENTS

The authors are grateful to CNPq (303525/2016-9, 305680/2015-3, 301486/2016-6 and 401689/2015-8), INCT-Bioanalitica, FAPEMA (Universal 00927/2016 and PRONEM 210383/2016), and FAPESP (2014/02163-7) for financial support.

REFERENCES

1. M. Cruz-Vera, R. Lucena, S. Cárdenas, and M. Valcárcel, *Trends Anal. Chem.* 28, 1164 (2009).
2. X. Gao, C. Xie, Y. Wang, Y. Luo, T. Yagai, D.S.X. Qin, K.W. Krausz, and F.J. Gonzalez, *Biochem. Pharmacol.* 119, 93 (2016).
3. N. Khan, H.N. Abdelhamid, J.Y. Yan, F.T. Chung, and H.F. Wu, *Anal. Chem. Res.* 3, 89 (2016).
4. A. Legendre, S. Jacques, F. Dumont, J. Cotton, P. Paullier, J.M. Fleury, and E. Leclerc, *Toxicol. In Vitro* 28, 1075 (2014).
5. L.J.N. Vergara, D. Farias, S. Bollo, and J.A. Squella, *Bioelectrochemistry* 53, 103 (2001).
6. N. Khan, H.N. Abdelhamid, J.Y. Yan, F.T. Chung, and H.F. Wu, *Anal. Chem. Res.* 3, 89 (2015).
7. M.J. Chaichi, S.N. Azizi, and M. Heidarpour, *Spectrochim. Acta Mol. Biomol. Spectrosc.* 116, 594 (2013).
8. H.R. Salgado, M. Menezes, and M.P.B. Storti, *Acta Farm. Bonaer.* 24, 246 (2015).
9. D. Merli, S. Protti, M. Labo, M. Pesavento, and A. Profumo, *Talanta* 151, 119 (2016).
10. J. Wang, *Electroanalysis* 3, 255 (1991).
11. R.W. Murray, *Electroanalytical Chemistry: A Series of Advances*, vol. 13, ed. A.J. Bard (New York: Marcel Dekker, 1984), p. 191.
12. S.M. Silva, L.F. Aguiar, R.M.S. Carvalho, A.A. Tanaka, F.S. Damos, and R.C.S. Luz, *Microchim. Acta* 183, 1251 (2016).
13. R.M. Oliveira, N.G. Santos, L.A. Alves, K.C.M.S. Lima, L.T. Kubota, F.S. Damos, and R.C.S. Luz, *Sens. Actuators B Chem.* 221, 740 (2015).
14. A. Rahi, K. Karimian, and H. Heli, *Anal. Biochem.* 497, 39 (2016).
15. P. Santhosh, K.M. Manesh, A. Gopalan, and K.P. Lee, *Sens. Actuators B Chem.* 125, 92 (2007).
16. M. Mazloum-Ardakani, H. Beitollahi, B. Ganjipour, H. Naeimi, and M. Nejati, *Bioelectrochemistry* 75, 1 (2009).
17. X.Q. Lin, J.B. He, and Z.G. Zha, *Sens. Actuators B Chem.* 119, 608 (2006).
18. H. Dai, Y. Wang, X. Wu, L. Zhang, and G. Chen, *Biosens. Bioelectron.* 24, 1230 (2009).
19. D. Ragupathy, A.I. Gopalan, and K.P. Lee, *Sens. Actuators B Chem.* 143, 696 (2010).
20. J. Zhang, X. Tan, D. Zhao, S. Tan, Z. Huang, Y. Mi, and Z. Huang, *Electrochim. Acta* 55, 2522 (2010).
21. R.T. Kachoosangi, G.G. Wildgoose, and R.G. Compton, *Anal. Chim. Acta* 618, 54 (2008).
22. K.J. Huang, X. Liu, W.-Z. Xie, and H.X. Yuan, *Colloids Surf. B Biointerfaces* 64, 269 (2008).
23. R.N. Goyal, A. Tyagi, N. Bachheti, and S. Bishnoi, *Electrochim. Acta* 53, 2802 (2008).
24. A. Afkhami, H. Ghaedi, T. Madrakian, D. Nematollahi, and B. Mokhtari, *Talanta* 121, 1 (2014).
25. B. Dogan-Topal, B. Bozal-Palabıyık, B. Uslu, and S.A. Ozkan, *Sens. Actuators B Chem.* 177, 841 (2013).
26. M. Taei and F. Abedi, *Chin. J. Catal.* 37, 436 (2016).
27. H. Beitollahi, M.A. Taher, M. Ahmadipour, and R. Hosseinzadeh, *Measurement* 47, 770 (2014).
28. M. Amiri-Aref, J.B. Raoof, and R. Ojani, *Colloids Surf. B Biointerfaces* 109, 287 (2013).
29. A.A. Ensafi, H. Bahrami, H. Karimi-Maleh, and S. Mallakpour, *Chin. J. Catal.* 33, 1919 (2012).
30. A. Mokhtari, H. Karimi-Maleh, A.A. Ensafi, and H. Beitollahi, *Colloids Surf. B Biointerfaces* 169, 96 (2012).
31. B. Rezaei and S.Z.M. Zare, *Sens. Actuators B Chem.* 134, 292 (2008).
32. M. Torkashvand, M.B. Gholivand, and G. Malekzadeh, *Sens. Actuators B Chem.* 231, 759 (2016).
33. T. Thomas, R.J. Mascarenhas, O.J. D'Souza, P. Martis, J. Dalhalle, and B.E.K. Swamy, *J. Colloid Interface Sci.* 402, 223 (2013).
34. V. Rajeev Jain, *Colloids Surf. B Biointerfaces* 87, 423 (2011).

35. M.M. Khalil and G.M. Abed El-aziz, *Mater. Sci. Eng. C* 59, 838 (2016).
36. H. Zanin, C.M.R. Rosa, N. Eliaz, P.W. May, F.R. Marciano, and A. Lobo, *Nanoscale* 7, 10218 (2015).
37. H. Zanin, P.W. May, A.O. Lobo, E. Saito, J.P.B. Machado, G. Martins, V.J. Trava-Airoldi, and E.J. Corat, *J. Electrochem. Soc.* 161, H290 (2014).
38. H. Zanin, A.M. Ferreira, N.S. Silva, F.R. Marciano, E.J. Corat, and A.O. Lobo, *Mater. Sci. Eng. C Biomim. Sens. Syst.* 41, 65 (2014).
39. J.V.S. Moreira, E.J. Corat, P.W. May, L.S.D. Cardoso, P.A. Lelis, and Z. Hudson, *J. Electron. Mater.* 45, 5781 (2016).
40. C.J.H. Adler, A. Hurley, and F.G. Strathmann, *Clin. Biochem.* 47, 80 (2014).
41. N. Laube, B. Mohr, and A. Hesse, *J. Cryst. Growth.* 233, 367 (2001).
42. G.V.S. Reddy, C.L.N. Reddy, V.N.E. Myreddy, and S.J. Reddy, *J. Clin. Med. Res.* 3, 35 (2011).
43. R.C.S. Luz, F.S. Damos, A.B. Oliveira, J. Beck, and L.T. Kubota, *Talanta* 64, 935 (2004).
44. K.C.M.L. Soares, A.C.F. Santos, R.N. Fernandes, F.S. Damos, and R.C.S. Luz, *Microchem. J.* 128, 226 (2016).
45. V. Mirčeski and M. Lovrić, *J. Electroanal. Chem.* 497, 114 (2001).
46. Analytical Methods Committee, *Analyst* 112, 199 (1987).
47. F. Ahmadi, J.B. Raoof, R. Ojani, M. Baghayeri, M.M. Lakouraj, and H. Tashakkorian, *Chin. J. Catal.* 36, 439 (2015).
48. P.K. Brahman, R.A. Dar, and K.S. Pitre, *Arab. J. Chem.* 9, S1884 (2016).
49. P.K. Brahman, R.A. Dar, S. Tiwari, and K.S. Pitre, *Colloids Surf. A Physicochem. Eng. Asp.* 396, 8 (2012).
50. A.A. Ensafi, E. Khoddami, and B. Rezaei, *J. Iran. Chem. Soc.* 13, 1683 (2016).
51. A.A. El-Shanawany, S.M. El-Adl, D.S.A. El Haleem, and S.A. El Wanees, *Ann. Chem. Forsch.* 2, 29 (2014).
52. H.N. Deepakumari and H.D. Revanasiddappa, *ISRN Spectrosc.* 2012, 1 (2012).